Light-Promoted Minisci Coupling Reaction of Ethers and Aza Aromatics Catalyzed by Au/TiO$_2$ Heterogeneous Photocatalyst

Zhanchong Li,[a] Liangying Wu,[a] Jiabao Guo,[a] Yifei Shao,[a] Yang Song,[a] Yuzhou Ding,[b] Li Zhu,[b] and Xiaoquan Yao*[a]

In this paper, Au/TiO$_2$ nanocomposite was synthesized and utilized as highly efficient and green photocatalyst for organic reactions. A sheet-like anatase titanium dioxide material with a highly active (001) crystal plane was prepared via a solvothermal method. Gold nanoparticles were then loaded on the surface of TiO$_2$ by a liquid-phase reduction method to give an Au/TiO$_2$ material with good photocatalytic activity. The Au/TiO$_2$ nanocomposite was utilized as a photocatalyst to develop a light-promoted Minisci oxidative coupling reaction of ether and aza aromatics by using oxygen as green oxidant and only catalytic amount of acid as additive. The protocol shows a good functional group tolerance as well as good to excellent yields for various substrates. With mechanistic studies, Au/TiO$_2$ nanocomposite proved to be an efficient photocatalyst to activate C—H bond via a SEO approach of heteroatoms. Moreover, the solid semiconductor photocatalyst shows good recycling performance, could be easily recovered and reused without significant decrease in yield.

Introduction

Sunlight, due to its abundance, absence of cost, and eco-friendly nature, possesses great potential in driving environmentally benign organic transformations.[1] Developing clean, sustainable and economically viable chemical technologies has attracted extensive researches. Photoredox catalysis has recently emerged as a powerful tool for the functionalization of C—H and C—X bonds, which undergoes single-electron transfer (SET) pathway to selectively construct C—C bonds.[2] The most common utilized photosensitizers such as ruthenium or iridium complexes and metal free organic dyes act as single-electron donors or acceptors in their excited states.[3] However, heterogeneous photocatalysis has been seen less use in organic transformations.[4]

Among varies of semiconductor photocatalysts, titanium dioxide (TiO$_2$) is undoubtedly the most promising materials for their numerous and diverse applications, which ranges from sunscreens, photovoltaic cells, to a series of environmental and biomedical applications, such as photocatalytic degradation of pollutants, water purification, biosensing, and drug delivery.[5] To date, limited by titania's low quantum efficiency and high band gap (3.0~3.2 eV, located at the ultraviolet (UV) wavelength range), utilizing mesoporous titania as highly active photocatalysts, however, remains challenging.[6] Embedding noble-metal nanoparticles is considered as an efficient approach to improve the photocatalytic activity of TiO$_2$ by enhancing quantum efficiency and visible-light adsorption, which recently intrigues many researchers' interests.[7]

Furthermore, although titanium dioxide can be used as a photocatalyst to achieve organic conversions especially in a photodegrade process, there are only very limited examples for its utilization in a practical synthetic process, especially for C—C bond coupling reaction based on C—H activation.[8]

On the other hand, the C—H functionalization of heterocycle compounds is worthwhile a long-term topic to pay attention to, because of their intrinsic versatility and unique physicochemical properties. Among the reported methodologies, Minisci reaction, pioneered by Minisci in 1971,[9] is a specific type of reaction involving the addition of radical species and electron-deficient heteroarenes, and great efforts have been made to explore the method of initiating free radical from radical precursors.[10]

Traditionally, stoichiometric peroxides & high temperatures were required to initialize free radicals in the reaction (Scheme 1a), which to some extent limits the selectivity of substrates and the tolerance of ethers.[11] During the last decade, an increasing amount of researches focus on a milder and greener protocol via photoredox pathway (Scheme 1b).[12] McMillan and co-workers first reported a visible light-mediated CDC with an iridium photocatalyst [Ir(dF(CF$_3$)ppy)$_2$(dtbbpy)]PF$_6$ at room temperature (Scheme 1b, (1)).[12a] Ryu's group employed decatungstate photocatalyst TBATD as both photosensitizer and hydrogen atom abstractor for the reaction under solar light irradiation (Scheme 1b, (2)).[12b] With diacetyl as a traceless and sustainable photosensitizer, Li's group described the first ketone-enabled cross-dehydrogenative Minisci alkylation (Sche-

[a] Z. Li, L. Wu, J. Guo, Y. Shao, Y. Song, Prof. X. Yao
Department of Applied Chemistry
College of Material Science and Technology
Nanjing University of Aeronautics and Astronautics
Nanjing 210016 (P. R. China)
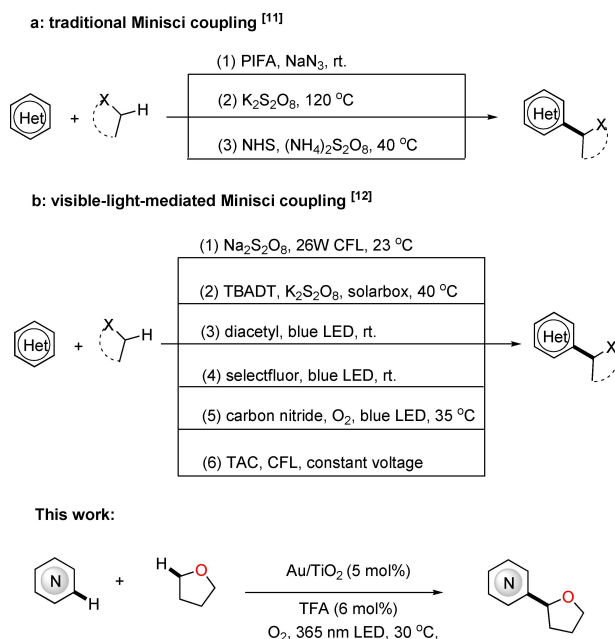E-mail: yaoxq@nuaa.edu.cn
[b] Y. Ding, L. Zhu
Department of Chemistry
School of Pharmacy
Nanjing Medical University
Nanjing 211166 (P. R. China)

me 1b, (3)).[12c] Moreover, Lei et al. discovered that Selectfluor, as the hydrogen atom abstractor, could form an N-centered radical cation following the blue-light-induced N–F activation of Selectfluor (Scheme 1b, (4)).[12d] Reisner's group recently achieved the Minisci reaction elegantly using a cyanamide functionalized carbon nitride as the photocatalyst and aerobic oxygen as the oxidant (Scheme 1b, (5)).[12e] It is regrettable that these aforementioned strategies mostly require expensive and potentially toxic Ir complex as photocatalyst and stoichiometric amount of strong peroxide or fluorine reagent as the hydrogen atom abstractor. Besides, the excessive amount of acid added, and high temperature limit the yield of certain method and the

tolerance of the substrates. To develop an environmentally-friendly and green methodology is still under investigation.

Herein, we hope to report an Au/TiO_2 nanocomposite catalyzed, light-promoted Minisci coupling reaction of ethers and aza aromatics. In this paper, a sheet-like anatase titanium dioxide material with a highly active (001) crystal plane was prepared via a solvothermal method. And then, gold nanoparticles were loaded on the surface of TiO_2 by a liquid-phase reduction method to give an Au/TiO_2 material. With the nanometric semiconductor as photocatalyst, a light-mediated Minisci coupling of N-heteroarenes and ethers was developed under the light of 365 nm LED in the presence of oxygen. The reaction shows a good functional group tolerance as well as good to excellent yields for various substrates. Moreover, the solid semiconductor photocatalyst has good recycling performance, and could be easily recovered and reused without significant decrease in yield.

Results and Discussion

Characterization studies

In the current work, anatase-type titanium dioxide with a rectangular sheet structure of uniform size was synthesized with tetrabutyl titanate as precursor by a solvothermal method. Gold nanoparticles were then loaded on the titanium dioxide by liquid-phase reduction to achieve the desired Au/TiO_2 material.

Figure 1 are transmission electron microscope images (TEM) of Au/TiO_2 photocatalytic material. It can be seen from Figure 1a that the gold nanoparticles are uniformly distributed on the surface of the titanium dioxide crystal, and the size of the gold nanoparticles is about 10 nm. The TiO_2 material is composed of a well-defined rectangular flake structure with a side length of
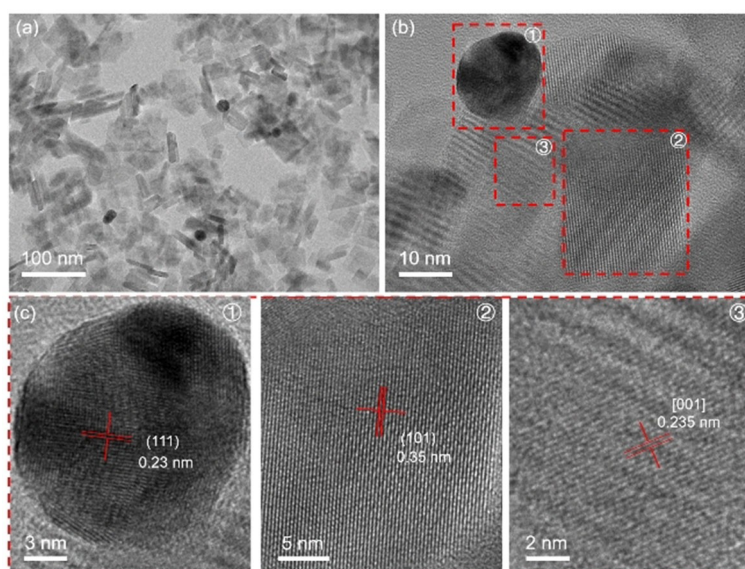
Scheme 1. Minisci coupling of heteroarenes and ethers.

Figure 1. (a) Typical TEM images and (b, c) high-resolution TEM images of Au/TiO_2.

about 40 nm and a thickness of about 6 nm. More specific structures of Au/TiO$_2$ are revealed in high resolution transmission electron microscopy (HRTEM) images (Figures 1b and 1c). The lattice spacing of metal particle in area ① is 0.23 nm, corresponding to the (111) plane of Au. Meanwhile, the lattice spacing of flake in area ② is 0.35 nm, attributing to the (101) plane of anatase TiO$_2$, which is consistent with the XRD analysis result. The lattice spacing in area ③ is 0.235 nm, which is indexed to the (001) plane of TiO$_2$.

The phase and crystal structure of TiO$_2$ and Au/TiO$_2$ photocatalytic material were investigated by the X-ray diffraction (XRD) as shown in Figure 2. In Figure 2a, there are 5 strong diffraction peaks located at 25.3°, 37.8°, 48.1°, 53.9° and 55.1° in as-synthesized TiO$_2$, corresponding to (101), (004), (200), (105) and (211) planes of anatase TiO$_2$ (JCPDS: 21-1272), respectively. In Figure 2b, except for the peaks of gold (JCPDS: 4-784) and anatase titanium dioxide, no other XRD diffraction peaks appeared in Au/TiO$_2$, indicating that the addition of gold did not change the crystal form of titanium dioxide. Moreover, it could be found that the peak of the gold element in Au/TiO$_2$ is weak, which may be caused by the low loading of gold. The result of the ICP test shows that the loading amount of gold element in the material is 4.98%. No new peak appears after the noble metal Au is embedded, which suggests that the synthesized composite catalyst material has no lattice distortion.

Figure 3 shows the XPS analysis of the TiO$_2$ material and Au/TiO$_2$ nanocomposite. For comparison, the Ti 2p and O 1s high-resolution spectra of TiO$_2$ are shown in Figure 3a and 3b. The Ti 2p spectrum could be deconvoluted into four peaks, namely Ti^{3+}2p$_{3/2}$ (458.61 eV), Ti^{4+}2p$_{3/2}$ (459.01 eV), Ti^{3+}2p$_{1/2}$ (464.20 eV), Ti^{4+}2p$_{1/2}$ (464.94 eV), which proves that Ti^{3+} is doped in the material.[13] By fitting the O 1s spectrum, two peaks could be obtained. In addition to the peak of O 1s (529.95 eV), there is a wider peak located at 531.36 eV, which is caused by oxygen vacancies. In order to maintain the electrical neutrality of the material, whenever two Ti^{3+} appear, an oxygen vacancy will appear. O$_{vac}$ and Ti^{3+} in the material would also inhibit the recombination of photogenerated carriers to a certain extent.[14]

To further illustrate the successful loading of Au nanoparticles on TiO$_2$, XPS characterization was also performed on Au/TiO$_2$ composite samples. In the survey spectrum (Figure 3c), in addition to the standard peak of C 1s, there are also peaks of Au, Ti and O. In the high-resolution spectrum of Au 4f

(Figure 3d), there are two peaks at 83.33 eV and 86.91 eV, corresponding to the binding energy of Au 4f$_{7/2}$ and Au 4f$_{5/2}$, respectively.[15] As for the high-resolution spectrum of Ti 2p in Figure 3e, Ti 2p spectrum could be fitted into four peaks, namely Ti^{3+}2p$_{3/2}$ (458.33 eV), Ti^{4+}2p$_{3/2}$ (458.65 eV), Ti^{3+}2p$_{1/2}$ (463.85 eV), Ti^{4+}2p$_{1/2}$ (464.67 eV), it can be proved that the material is doped with Ti^{3+}. Compared with pure titanium dioxide material, the characteristic peak of Ti 2p shifts to the low-energy region, which may be due to the loading of gold nanoparticles causing electrons to move to titanium dioxide. Besides, in O 1s spectrum, it is found that, like the pure titanium dioxide material, in addition to the peak of O 1s (529.71 eV), there is a wider peak at 530.99 eV. Compared with TiO$_2$, it is more in the direction of the low energy region, which may be due to the decrease in the binding energy of Ti–O.[16]

Figure 4a is the UV-vis diffuse reflectance spectroscopy test (DRS) of TiO$_2$ and composite Au/TiO$_2$ catalyst materials. It can be seen from Figure 4a that compared with pure anatase TiO$_2$ material, Au/TiO$_2$ composite photocatalytic material has a more obvious absorption broadening in the visible light region (400-800 nm), and the absorption bandredshift. The results can prove that the local surface plasma effect of Au nanoparticles can increase the material's absorption of visible light and improve the light absorption of the composite material, so that the composite material has better photocatalytic activity. In addition, through the formula E$_g$ = 1240/λ, it can be deduced that the band gap of Au/TiO$_2$ is 2.95 eV, which is significantly shorter than the band gap of 3.2 eV of anatase TiO$_2$.

According to the diffuse reflectance spectrum, the Tauc plots of the two materials can be obtained, as shown in Figure 4b. It can be seen in the figure that Au/TiO$_2$ has a smaller optical band gap.

Fluorescence analysis was performed on the prepared anatase TiO$_2$ and Au/TiO$_2$ composite materials to characterize the recombination efficiency of photogenerated carriers. The experiment was performed at an excitation wavelength of 300 nm, and the results are summarized in Figure 5a. It can be seen from Figure 5a that the fluorescence emission intensity of the TiO$_2$ material is greater, indicating that the recombination efficiency of its photogenerated carriers is higher. The low fluorescence emission intensity of Au/TiO$_2$ composite material proves the low recombination efficiency of photogenerated carriers. This is due to the migration of Au nanoparticles to photogenerated electrons, which strongly inhibits the recombination of photogenerated carriers. It might indicate that the composites possessed higher photocatalytic activity under visible light irradiation than TiO$_2$.

Figure 5b is the Mott-Schottky curve of the two materials. Knowing that C = 1/ωZ$_i$, plot 1/C^2 with potential to get the Mott-Schottky curve. According to calculations, the corresponding slopes of the two materials TiO$_2$ and Au/TiO$_2$ are 2.262 and 1.746 respectively. The slope is positive, which proves that the two materials prepared are all n-type semiconductors. And the slope of the Au/TiO$_2$ material is the smallest, which means the concentration of photogenerated carriers is the highest.
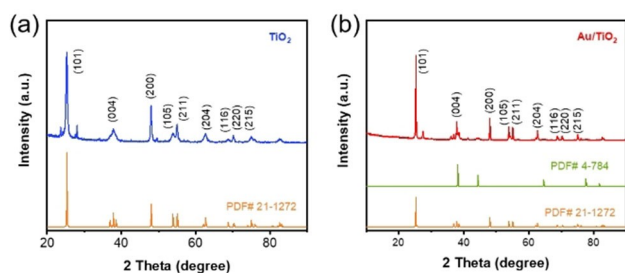

Figure 2. (a) XRD patterns of TiO$_2$ and (b) Au/TiO$_2$.

ChemCatChem

Full Papers
doi.org/10.1002/cctc.202100298

**Chemistry
Europe**

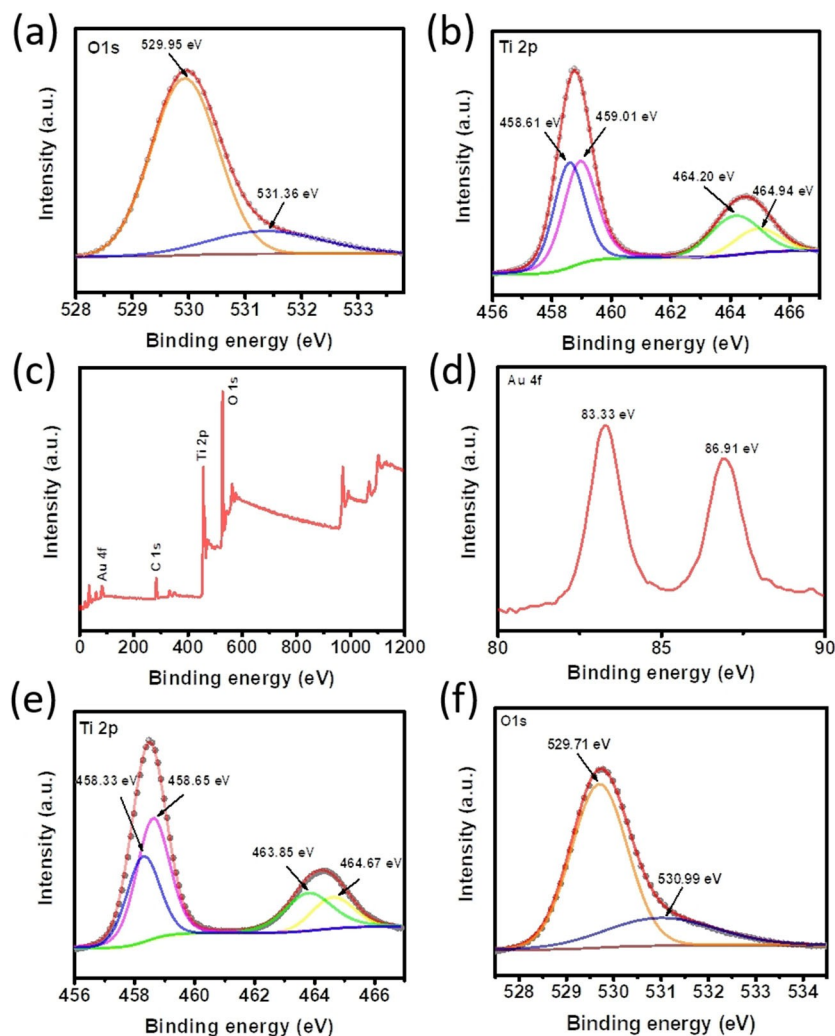European Chemical
Societies Publishing

Figure 3. (a) Ti 2p high-resolution spectrum of TiO_2 material and (b) O 1s high-resolution spectrum, (c) XPS survey spectrum of Au/TiO_2 material, (d) high resolution spectrum of Au 4f, (e) high resolution spectrum of Ti 2p and (f) high resolution spectrum of O 1s.
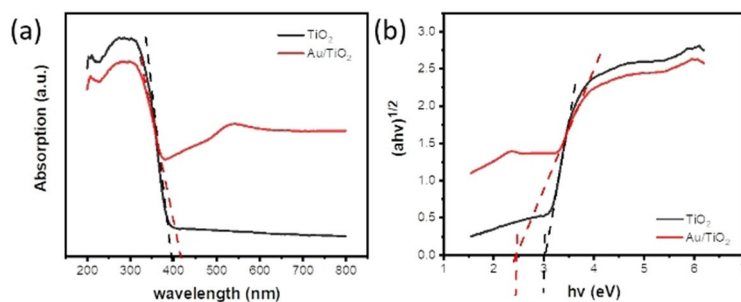

Figure 4. (a) UV-vis diffuse reflectance spectrum and (b) Tauc plots of TiO_2 and Au/TiO_2.

Minisci Coupling Catalyzed by Au/TiO_2

With Au/TiO_2 nanometric semiconductor as photocatalyst, we hope to explore an oxidative C—C coupling reaction based on a C—H bond activation, and Minisci reaction of ethers and aza

aromatics was selected. Our initial research focused on the model reaction of isoquinoline (**1a**) with THF (**2a**).

As given in Table 1, under the light of 365 nm from a 6 W LED, the coupling product was isolated with a 95% yield by using Au/TiO_2 as the photocatalyst at 30°C under oxygen atmosphere in the presence of catalytic amount of TFA (entry 1,
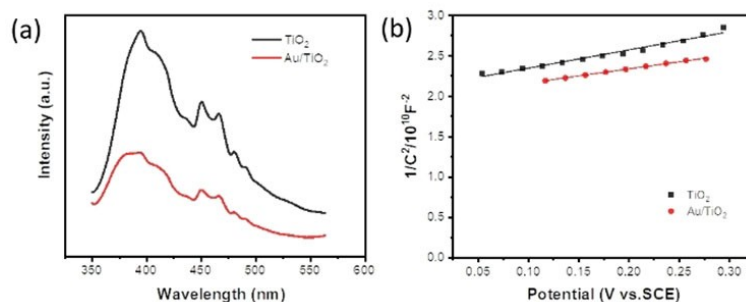
Figure 5. (a) Fluorescence spectra and (b) Mott-Schottky curves of TiO_2 and Au/TiO_2.

Table 1. Optimization of reaction conditions.[a]

Entry	Catalyst (mol%)	Addictive (mol%)	Yield[b] (%)
1	Au/TiO₂ (5)	TFA (6)	95
2	Au/C₃N₄ (5)	TFA (6)	N.R.
3	Ag/C₃N₄ (5)	TFA (6)	N.R.
4	TiO₂ (37 mg)	TFA (6)	75
5	Cu/TiO₂ (5)	TFA (6)	46
6	Ag/TiO₂ (5)	TFA (6)	59
7	Pt/TiO₂ (5)	TFA (6)	76
8	Pd/TiO₂ (5)	TFA (6)	64
9[c]	Au/TiO₂ (5)	TFA (6)	Trace
10[d]	Au/TiO₂ (5)+Eosin Y (100)	TFA (6)	Trace
11	Au/TiO₂ (5)	TFA (50)	72
12	Au/TiO₂ (5)	TFA (100)	53
13[e]	Au/TiO₂ (5)	TFA (6)	67
14[f]	Au/TiO₂ (5)	TFA (6)	95
15[g]	Au/TiO₂ (5)	TFA (6)	N.R.
16	–	TFA (6)	N.R.
17	Au/TiO₂ (5)	–	N.R.
18[h]	Au/TiO₂ (5)	TFA (6)	53

[a] Conditions: **1a** (0.2 mmol), **2** (2 mL), TFA, catalyst, oxygen atmosphere, irradiated by 365 nm LED, 30 °C, 24 h; [b] isolated yields; [c] 400 and 550 nm LED; [d] 455 nm LED; [e] **1a** (1 mL); [f] **1a** (3 mL); [g] in the dark; [h] in the air.
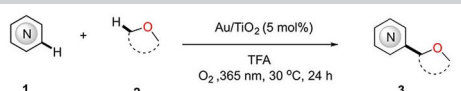
Table 1). Similar nanometric semiconductors based on C_3N_4 were also detected, and they were inert to the reaction under the same conditions (entries 2–3, Table 1). Next, we tested unmodified TiO_2 and other transition metal-modified TiO_2 (Cu, Ag, Pt, Pd), and the yields were reduced to varying degrees compared with Au/TiO_2 materials (entries 4–8 *vs.* entry 1, Table 1). When 400 nm or 550 nm LED utilized instead of 365 nm, there was only trace product obtained (entry 9, Table 1). With Eosin Y as co-catalyst, the reaction was also tried under blue light, but only trace reaction occurred (entry 10, Table 1).
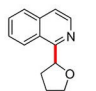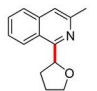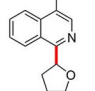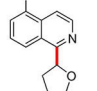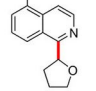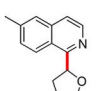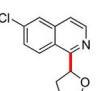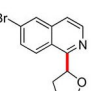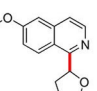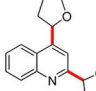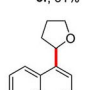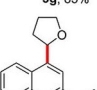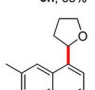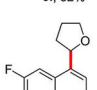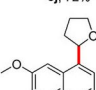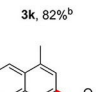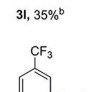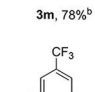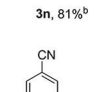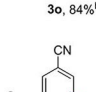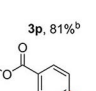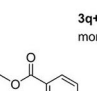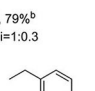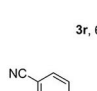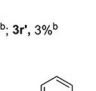
From a mechanistic standpoint, TFA was generally added to lower the heteroarene's electron density so as to facilitate the attack of nucleophiles.[10] However, increasing the loading of TFA led to the decline of the yield (entries 11–12, Table 1). We also examined the influence of substrate concentration, and 0.1 M of **1a** in THF was an appropriate condition (entries 13–14 *vs.* entry 1, Table 1). In the absence of light, photocatalyst or

TFA, no reactions occurred, respectively. It is obviously that the light, photocatalyst and TFA are all necessary in the current approach (entries 15–17, Table 1). Moreover, if the reaction was conducted in air, only a 53% yield was obtained (entry 18, Table 1), in which there was no H_2 production detected by GC analysis. The lower yield of the reaction conducted in the air probably was due to the high oxygen concentration required for the reaction.
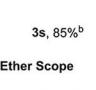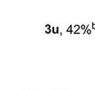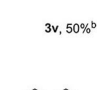
With the optimized conditions in hand, we next investigated the substrate scope (Table 2). As shown in Table 2, isoquinolines with electron-withdrawing and electron-donating groups all smoothly delivered the corresponding products in moderate to excellent yields (**3a**–**3i**). Quinoline derivatives were then detected in the reaction. Intriguingly, quinoline gave a di-substituted product at C-2 and C-4 position concurrently, which indicated that quinolines have two electrophilic sites (**3j**). Employing C-2 or C-4 blocked quinolines, exclusive regioisomers were formed with good yields in most examples (**3k**, **3m**–

These are not the final page numbers! ↗↗

Table 2. Scope of Minisci alkylation with ethers.

[a] Reaction conditions:**1** (0.2 mmol), **2** (2 mL), Au/TiO₂ (5 mol%), TFA (6 mol%), 365 nm LED, oxygen atmosphere, 30 °C, 24 h; isolated yield; [b] TFA (50 mol%); [c] THF (1 mL), DCM (1 mL).

Figure 6. The recyclability of the Au/TiO₂ photocatalyst in the Minisci reaction.

Figure 7. The "ON/OFF" experiment.

3p), except 2-phenylquinoline provided a relatively low yield, which might result from the steric hindrance of the phenyl group (**3l**). Additionally, various pyridines afforded corresponding two-component coupling products in good yields (**3q–3w**). Notably, 4-(trifluoromethyl)pyridine and 4-cyanopyridine could provide a major C-2 substituted product and the di-substituted at C-2&C-6 as by-product, respectively, while 3-cyanopyridine presented a regiospecfic at C-6 (**3q–3r**, **3v**). To our delight, good tolerance was displayed for both ethyl and ester derivatives with satisfied yields (**3s–3t**, **3u**, **3w**).

Some THF analogues were also evaluated in the reaction with isoquinoline as the coupling partner. 2-Meth-yltetrahydrofuran experienced C-2 heteroarylation selectively, maintaining a moderate yield of 67% (**4a**). For 1,3-dioxolane, compared with C-4 position, the reaction process favored C-2 position more, providing the desired products with the yield of 64% and 8%, respectively (**4b** and **4b'**). Moreover, tetrahydro-
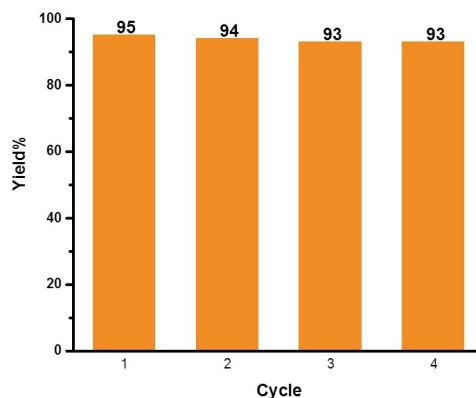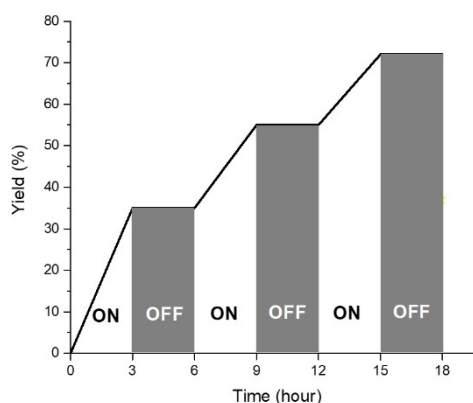
pyran also gave the corresponding coupling product in 65% yield (**4c**).

Having demonstrated the capacity of a variety of hetero-aromatics, we next examined the recyclability of Au/TiO₂, which represented a distinctive feature as a kind of heterogeneous photocatalyst. We could recover the catalyst easily from the reaction mixture by centrifugation. Then, the recycled material was utilized to perform the reaction with fresh substrates and additive again. It can be seen from Figure 6 that the catalyst still maintains a commendable photocatalytic performance after four cycles without significant drop in yield.

To further demonstrate the role of the photoirradiation, an "on/off" experiment was performed. According to the results in Figure 7, it can be seen that the reaction was temporarily interrupted in the absence of light and continued to work smoothly once under light irradiation. It clearly showed that the continuous excitation of light was required to realize the high activity of the photocatalyst, and it can also suggest that the mechanism of the reaction was not a free radical chain reaction.

In order to understand the mechanism of the reaction, two controlled experiments were designed and carried out (Scheme 2). Under the standard conditions, 2 equivalents of radical scavenger, TEMPO, was added, and the reaction was

These are not the final page numbers! ↗↗

ChemCatChem

Full Papers
doi.org/10.1002/cctc.202100298

Chemistry
Europe
European Chemical
Societies Publishing

then completely inhibited. Therefore, it indicated that the reaction should undergo a radical process (eq. 1, Scheme 2). In addition, 0.5 mL of THF was mixed with 10 mg of Au/TiO$_2$ photocatalyst alone and stirred for 24 h under light irradiation in O$_2$. A small amount of γ-butyrolactone (*ca.* 2%) could be separated, which suggested that the C−H bond at the α-position of THF could be activated effectively by the photocatalyst under the current conditions (eq 2, Scheme 2).
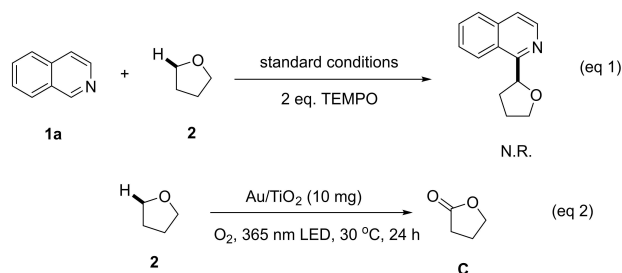
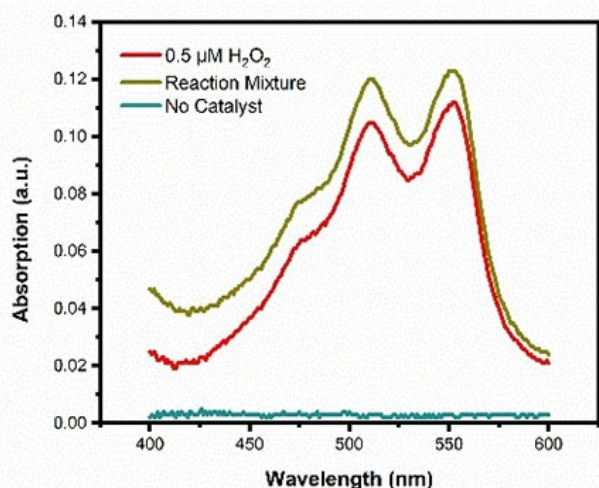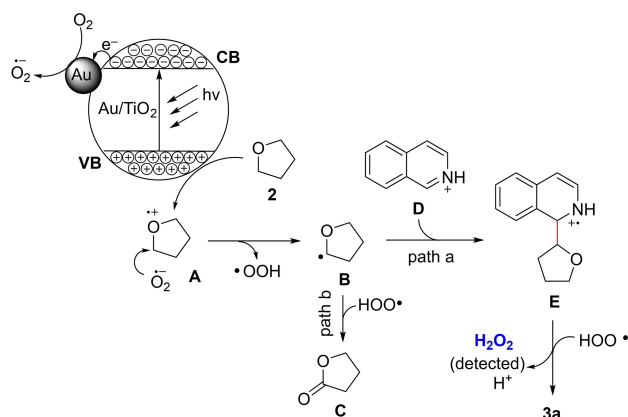**Scheme 2.** Control experiments for the mechanism investigation.

Figure 8. UV-vis absorption spectra of reaction aqueous extract after adding DPD and POD reagents for H$_2$O$_2$ determination.

Scheme 3. Proposed reaction mechanism.

Intriguingly, the formation of H$_2$O$_2$, which is one of the postulated intermediates in the aerobic oxidation reactions, was also detected through the oxidation of *N,N*-diethyl-1,4-phenylenediammonium sulphate (DPD) catalyzed by Horseradish peroxidase (POD). As shown in Figure 8, two absorption peaks centered at *ca.* 510 and 551 nm can be observed.[17] Also, no relevant signal peak was detected in the reaction mixture without catalyst, which confirmed that hydrogen peroxide was produced during the reaction (Figure 8).

Based on results above and the related literature, especially our previous reports on similar heterogeneous photocatalytic process,[4b,d, e,12a,c] a plausible mechanism was proposed in Scheme 3. Initially, after Au/TiO$_2$ composite material is excited by light, electrons transfer from the valence band to the conduction band (e$^-$), forming corresponding holes (h$^+$). Through the single electron oxidation between **2** and valence band holes (h$^+$), the free radical cation intermediate **A** is produced. On the other hand, conduction band electrons are entrapped to the surface of Au nanoparticles to reduce oxygen to superoxide radical anion. Subsequent hydrogen transfer between **A** and superoxide radical forms tetrahydrofuran α-position free radical intermediate **B** and hydrogen peroxide radicals. Following path a, radical **B** and protonated isoquinoline **D** undergo a radical addition reaction to obtain **E**; **E** then loses hydrogen atoms under the action of hydrogen peroxide radicals, and finally is deprotonated to give the target coupling product **3a**, while one molecule H$_2$O$_2$ was formed. Additionally, through path b, α-radical **B** combines with hydrogen peroxide radical to give γ-butyrolactone.[20]

Conclusion

In summary, uniform-sized gold nanoparticles were successfully supported on anatase-type titanium dioxide to prepare an Au/TiO$_2$ nanometric semiconductor material. The local plasma effect of gold nanoparticles and the unique semiconductor properties of titanium dioxide are combined to obtain a photocatalytic material with high activity and high light absorption properties. By using Au/TiO$_2$ as the photocatalyst, oxygen as oxidant, catalytic amount of TFA as the acidic additive, the oxidative coupling reaction of heteroaromatic compounds and cyclic ethers, known as Minisci reaction, was performed successfully under the irradiation of 365 nm LED. In this reaction, Au/TiO$_2$ nanocomposite proved to be an efficient photocatalyst to activate C−H bond via a SEO approach of heteroatoms. Further studies to elucidate additional mechanistic details and to apply this strategy to new organic transformation are ongoing in our laboratory.

Experimental Section

Preparation of TiO$_2$ nanosheets

Titanium dioxide material was prepared using classic solvothermal method.[18] 5 mL portions of tetrabutyl titanate and 0.6 mL hydro-

fluoric acid were put into a 25-mL Teflon-lined autoclave. The mixture was kept at 200 °C for 24 hours. After being naturally cooled to room temperature, it is centrifuged with a high-speed centrifuge, and the solid matter was washed with distilled water and ether for several times, and it was placed in a vacuum drying oven at 40 °C overnight. Finally, TiO_2 nanosheets was obtained as white powder.

Preparation of Au/TiO$_2$ nanocomposite

Au nanoparticles were prepared by the method of liquid-phase reduction.[19] 1.0000 g of the above-prepared titanium dioxide material was dispersed in 100 mL of distilled water. Then the mixture was ultrasonicated for 30 minutes, stirred for 30 minutes, and transferred to a 250 mL three-necked flask under the protection of a nitrogen atmosphere, consequently 4 mL of 0.025 mol L^{-1} HAuCl$_4$·3H$_2$O aqueous solution was added and stirred for 30 min, and then heated to boiling. Quickly add 40 mL of 1 wt% trisodium citrate dihydrate aqueous solution and reflux for 10 min under vigorous stirring. It can be observed that the solution turns dark purple. Then remove the heat source, continue stirring for 15 min, and let the solution cool to room temperature. Then the reaction system was centrifuged at high speed, washed with distilled water and ether several times, and the sample was placed in a vacuum drying oven at 40 °C to dry overnight to obtain purple Au/TiO$_2$ (5 wt%) material.

Typical procedures for the synthesis of 3&4

The reaction was performed with WATTCAS WP-TEC-1020H5L parallel reactor. Under oxygen atmosphere, Au/TiO$_2$ material 5 mol% (39.2 mg), isoquinoline **1a** (0.2 mmol), 6 mol% trifluoro-acetic acid (1 μL) and tetrahydrofuran **2a** (2 mL) were added into the thick-walled pressure-resistant quartz tube, which was sealed consequently. The reaction mixture was irradiated by 365 nm LED and stirred for 24 h at 30 °C. The reaction mixture was separated and purified by flash column chromatography on silica gel (hexanes: ethyl acetate = 3 : 1), the product **3a** was a colorless liquid, and the yield was 95%. By the same method, other products **3b**–**3i** were synthesized. 50 mol% TFA is used to give **3j**–**3w** and **4a**–**4b**. Tetrahydropyran **2c** (1 mL) and DCM (1 mL) is used as solvent to obtain **4c**.

The detailed characterization data for compounds **3** and **4** are provided in Supporting Information.

Acknowledgements

Conflict of Interest

The authors declare no conflict of interest.

[1] D. Ravelli, M. Fagnoni, A. Albini, *Chem. Soc. Rev.* **2013**, *42*, 97–113.
[2] a) J. M. Narayanam, C. R. Stephenson, *Chem. Soc. Rev.* **2011**, *40*, 102–113; b) D. M. Schultz, T. P. Yoon, *Science* **2014**, *343*, 1239176; c) T. P. Yoon, M. A. Ischay, J. Du, *Nat. Chem.* **2010**, *2*, 527–532.
[3] C. K. Prier, D. A. Rankic, D. W. MacMillan, *Chem. Rev.* **2013**, *113*, 5322–5363.
[4] Recent review: a) H. Kisch, *Acc. Chem. Res.* **2017**, *50*, 1002–1010. Recent examples from other and our group:; b) A. Hainer, N. Marina, S. Rincon, P. Costa, A. E. Lanterna, J. C. Scaiano, *J. Am. Chem. Soc.* **2019**, *141*, 4531–4535; c) Y.-Y. Liu, D. Liang, L.-Q. Lu, W.-J. Xiao, *Chem. Commun.* **2019**, *55*, 4853–4856; d) L. Wang, M. Yu, C. Wu, N. Deng, C. Wang, X. Yao, *Adv. Synth. Catal.* **2016**, *358*, 2631–2641; e) P. Wang, X. Wang, X. Niu, L. Zhu, X. Yao, *Chem. Commun.* **2020**, *56*, 4840–4843.
[5] a) X. Chen, S. S. Mao, *Chem. Rev.* **2007**, *107*, 2891–2959; b) A. Fujishima, K. Honda, *Nature* **1972**, *238*, 37–38; c) H. Chen, C. E. Nanayakkara, V. H. Grassian, *Chem. Rev.* **2012**, *112*, 5919–5948; d) M. A. Henderson, I. Lyubinetsky, *Chem. Rev.* **2013**, *113*, 4428–4455; e) A. L. Linsebigler, G. Lu, J. T. Yates, *Chem. Rev.* **1995**, *95*, 735–758.
[6] U. I. Gaya, A. H. Abdullah, *J. Photochem. Photobiol. C* **2008**, *9*, 1–12.
[7] N. T. Nguyen, I. Hwang, T. Kondo, T. Yanagishita, H. Masuda, P. Schmuki, *Electrochem. Commun.* **2017**, *79*, 46–50.
[8] X. Lang, X. Chen, J. Zhao, *Chem. Soc. Rev.* **2014**, *43*, 473–486.
[9] a) R. Bernardi, F. Bertini, R. Galli, M. Perchinummo, F. Minisci, *Tetrahedron* **1971**, *27*, 3575–3579; b) C. Giordano, F. Minisci, E. Vismara, S. Levi, *J. Org. Chem.* **1986**, *51*, 536–537.
[10] M. A. J. Duncton, *MedChemComm* **2011**, *2*, 1135–1161.
[11] a) S. Ambala, T. Thatikonda, S. Sharma, G. Munagala, K. R. Yempalla, R. A. Vishwakarma, P. P. Singh, *Org. Biomol. Chem.* **2015**, *13*, 11341–11350; b) A. P. Antonchick, L. Burgmann, *Angew. Chem. Int. Ed. Engl.* **2013**, *52*, 3267–3271; c) S. Liu, A. Liu, Y. Zhang, W. Wang, *Chem. Sci.* **2017**, *8*, 4044–4050.
[12] a) J. Jin, D. W. MacMillan, *Angew. Chem. Int. Ed. Engl.* **2015**, *54*, 1565–1569; b) M. C. Quattrini, S. Fujii, K. Yamada, T. Fukuyama, D. Ravelli, M. Fagnoni, I. Ryu, *Chem. Commun.* **2017**, *53*, 2335–2338; c) C.-Y. Huang, J. Li, W. Liu, C.-J. Li, *Chem. Sci.* **2019**, *10*, 5018–5024; d) X.-A. Liang, L. Niu, S. Wang, J. Liu, A. Lei, *Org. Lett.* **2019**, *21*, 2441–2444; e) A. Vijeta, E. Reisner, *Chem. Commun.* **2019**, *55*, 14007–14010; f) H. Huang, Z. M. Strater, T. H. Lambert, *J. Am. Chem. Soc.* **2020**, *142*, 1698–1703.
[13] T.-S. Yang, M.-C. Yang, C.-B. Shiu, W.-K. Chang, M.-S. Wong, *Appl. Surf. Sci.* **2006**, *252*, 3729–3736.
[14] J. Li, H. C. Zeng, *Chem. Mater.* **2006**, *18*, 4270–4277.
[15] Y. Wu, J. Zhang, L. Xiao, F. Chen, *Appl. Catal. B* **2009**, *88*, 525–532.
[16] G. R. Bamwenda, S. Tsubota, T. Nakamura, M. Haruta, *J. Photochem. Photobiol. A* **1995**, *89*, 177–189.
[17] C. Su, M. Acik, K. Takai, J. Lu, S. J. Hao, Y. Zheng, P. Wu, Q. Bao, T. Enoki, Y. J. Chabal, K. P. Loh, *Nat. Commun.* **2012**, *3*, 1298.
[18] X. Han, Q. Kuang, M. Jin, Z. Xie, L. Zheng, *J. Am. Chem. Soc.* **2009**, *131*, 3152–3153.
[19] C. Y. Nan, Y. Zhang, Y. F. Li, Y. C. Zhao, *Univ. Chem. Educ.* **2019**, *34*, 58–63.
[20] We also calculated the quantum yield of the photocatalytic process under the optimal conditions, please see Part 2 in SupportingInforma-tion.

FULL PAPERS

Photocatalyzed Minisci coupling:
Au/TiO$_2$ nanometric semiconductor
was synthesized and utilized as a
highly efficient photocatalyst for
Minisci coupling reaction of heteroar-
omatic compounds and cyclic ethers
under 365 nm LED irradiation in
oxygen. Good functional group
tolerance as well as good to
excellent yields for various substrates
were achieved. Moreover, the solid
semiconductor photocatalyst
showed good recycling performance,
and could be easily recovered and
reused without significant decrease
in yield.
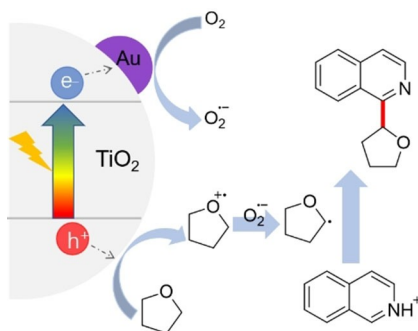
Z. Li, L. Wu, J. Guo, Y. Shao, Y. Song, Y. Ding, L. Zhu, Prof. X. Yao*

1 – 9

**Light-Promoted Minisci Coupling
Reaction of Ethers and Aza
Aromatics Catalyzed by Au/TiO$_2$
Heterogeneous Photocatalyst**